



Research paper

Automatic Detection of Lung Nodules on Computer Tomography Scans with a Deep Direct Regression Method

Khadijeh Aghajani*

Department of Computer Engineering, University of Mazandaran, Babolsar, Iran.

Article Info

Article History:

Received 02 December 2021

Revised 26 December 2021

Accepted 05 February 2022

DOI:10.22044/jadm.2022.11431.2303

Keywords:

Lung Nodule detection, Direct Regression, Deep Learning.

Corresponding

kh.aghajani@umz.ac.ir
Aghajani).

author:

(Kh.

Abstract

Deep-learning-based approaches have been extensively used in detecting pulmonary nodules from computer tomography (CT) scans. In this work, an automated end-to-end framework with a convolution network (Conv-net) is proposed to detect lung nodules from the CT images. Here, boundary regression has been performed by a direct regression method, in which the offset is predicted from a given point. The proposed framework has two outputs; a pixel-wise classification between nodule or normal and a direct regression that is used in order to determine the four coordinates of the nodule's bounding box. The loss function includes two terms; one for classification and the other for regression. The performance of the proposed method is compared with YOLOv2. The evaluation is performed using the Lung-Pet-CT-DX dataset. The experimental results show that the proposed framework outperforms the YOLOv2 method. The results obtained demonstrate that the suggested framework possesses high accuracies of nodule localization and boundary estimation.

1. Introduction

Lung cancer is still one of the most common causes of death worldwide in both men and women, while early screening of smaller nodules can significantly reduce lung cancer mortality and prolong the patient's life [1]. One of the most common approaches for early detection is the Computed Tomography (CT) analysis. The computer-aided detection systems can help the radiologists to focus on the regions of interest instead of finding nodules from hundreds of CT slices. In the following, we will review some research works carried out in this field. It should be noted that it is very difficult to compare various methods because they may use different databases or different annotation mechanisms.

Traditionally, the lung nodule detection methods are based on hand-crafted feature extraction using various image filters and a machine learning-based method to reduce false positives (FPs). The shape-based feature descriptors [2, 3], texture characteristics [3-5], multiscale Laplacian of Gaussian filtering [6], wavelet features [7], and curvedness features [8], are examples of the

common methods used in this field. In the traditional methods, the number of FPs is very high for each scan; thus a classifier such as support vector machine (SVM), random forest (RF), or k-nearest neighbors (k-NN) can be used to reduce FPs [3,4,8,9]. Moreover, in the traditional methods, the designed filters may not deal with all scale and shape variability of the nodules.

Recently, deep-learning-based approaches using convolutional neural networks (CNNs) can perform an end-to-end detection and learning salient features. Combining CNN and fully connected layers can be used to detect lung nodules [10-13]. Such methods overcome the problem of filter designing for extracting hand-crafted features and large FPs.

Recently, the application of deep learning-based object detection methods in nodule detection has received much attention. The following is a brief introduction to them and their application in this field. Region-based convolutional neural network (r-CNN) [14], fast r-CNN [15], and faster r-CNN

[16] are the popular methods for object detection. In r-CNN, using the selective search, the category-independent region proposals are created. Then the region proposals are fed into a CNN, and a feature vector is extracted from each region. Finally, the extracted features are fed into an SVM to filter out FPs. In fast r-CNN, the entire image and the region proposals are fed into a CNN, and SVM is replaced with a soft-max layer. In the faster r-CNN, a neural network-based region proposal is suggested and the results obtained are fed into a CNN after using an attention mechanism. Moreover, mask r-CNN is used for segmentation. It is developed on top of the faster r-CNN, so that along with the class label and bounding box offset, the object mask (that is a binary image) is considered [17]. In [18], the r-CNN-based method has been utilized for lung nodule detection. Ding et al. have utilized a faster r-CNN-based method to detect the initial nodule candidates followed by a CNN to reduce FPs [19]. The faster r-CNN has also been used in [20-25] to detect lung nodules. Some studies have used mask r-CNN to detect nodules and segment them [26, 27]. In [28], a modified faster r-CNN has been proposed to detect lung nodules. First, the image is fed into VGG16 with a de-convolutional layer. Then the obtained features are sent to the region proposal network (RPN) to generate the initial nodule candidates. Finally, the candidate region along with the convolutional features are fed into the region of interest (ROI) pooling layer followed by a multi-task classifier to position the regression of the candidate area.

Xie et al. have proposed a model consisting of a faster r-CNN along with two RPNs and a deconvolution layer for detecting the nodule candidates [22]. They utilized a 2D CNN-based boosting architecture to reduce FPs. Cue et al. have proposed a framework consisting of a cascaded r-CNN and a feature pyramid network (FPN) to detect lung nodules [29]. They used a residual neural network (ResNet) as the background network to extract the salient features. Another popular deep learning-based object detector is the YOLO algorithm, in which the multiple bounding boxes along with their class probabilities are predicted by a single CNN. YOLO and its variants have been used in some studies to detect lung nodules. George et al. have used YOLO [30], Xinzheng et al. have used YOLO-V2 [31] and Haibo et al. have

utilized YOLO-V3 [32] to detect lung nodules. It has been reported that such methods achieve a low accuracy in detecting small nodules.

In this paper, a direct-regression-based approach was utilized to generate the bounding box of the lung nodule. In such approaches, the regression task is learned to generate an object's position and size from a given point [33]. Briefly, the proposed framework can be subdivided into the following steps:

- Preprocessing: the goal of this step is to remove the irrelevant parts of the image and reduce the size of the image without losing important information.
- Generating the ground truth for the classification and regression tasks according to the annotation information and the proposed model. In this method, the distance of each pixel located in the positive area to the coordinates of the quadrilateral corners containing the nodule is learned. The loss function includes two terms; one for classification and the other for regression.
- Training the proposed CNN-based model by minimizing the loss function. In the proposed model, the features extracted from different scales are fused in order to deal with various scale and shape variability.

The proposed model has been evaluated on the Lung-Pet-CT-DX dataset [34]. This data contains 12984 CT scans belonging to 235 patients. Each scan contains one nodule identified by the experts. The position of the nodule is annotated. According to the studied papers, it seems that no report of the use of this data has been seen in this field. The performed experiments show that the proposed framework can detect most of the nodules correctly.

The organization of the rest of the paper is as follows. In Section 2, the pre-processing and the proposed deep learning architecture are presented. Section 3 is devoted to the experimental results. In Section 4, the conclusion is presented.

2. Main Idea and Proposed Method

In this section, the data preprocessing and the proposed framework are presented. First, a segmentation method is used in order to remove the background and irrelevant parts of the images.

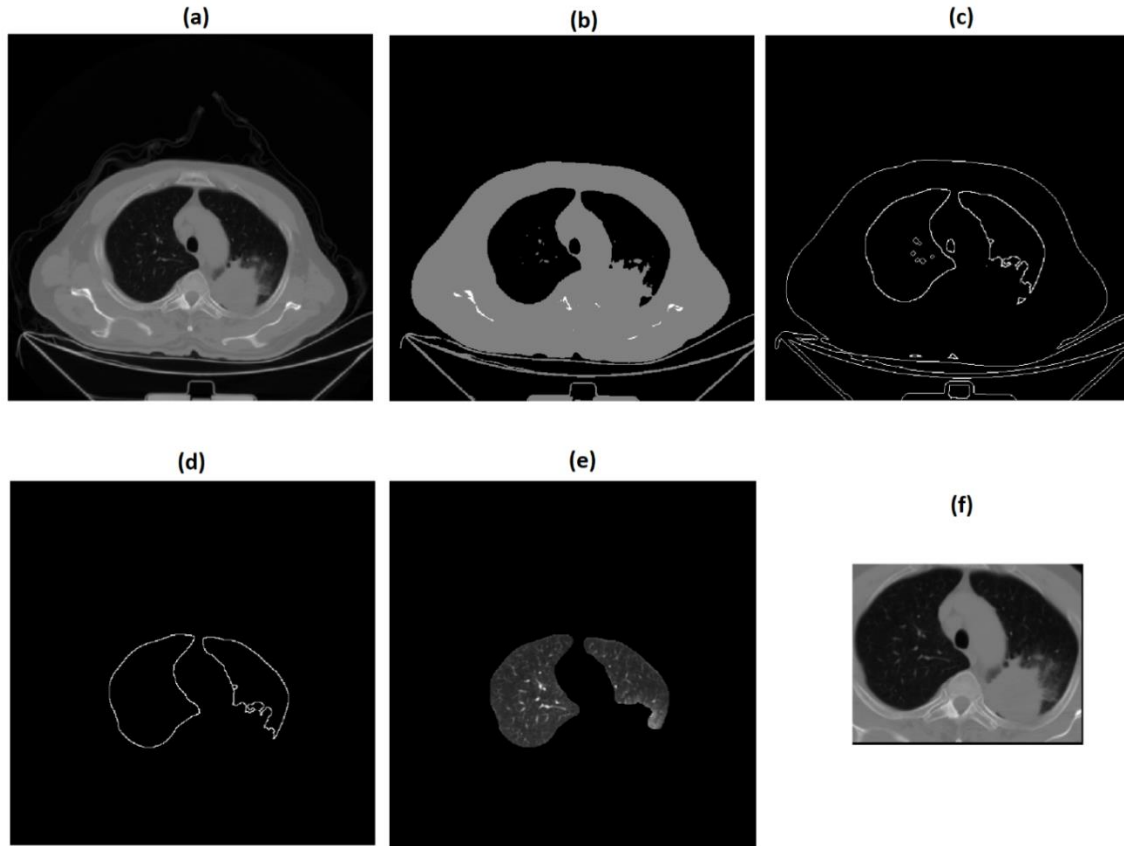


Figure 1. Example of lung corpus extraction. a) Original CT scan, (b) Bit-plane image (output of OR-ing bit number 7 and bit number 8), c) Output of outlining method, d) Refined extracted border, e) Extracted lung region that is obtained by multiplying the original image by flood fill image, f) Obtained corpus.

Since there is no need to consider the removed area for a later computation, it can facilitate nodule detection. The aim of preprocessing is to reduce the size of the images without losing important information. Here, a bit-plane-based segmentation method is utilized. In this method, the value of each pixel is converted to an 8-bit unsigned integer. A bit plane image is created by OR-ing the bit number 8 and bit number 7. After applying a threshold on the obtained image, a sequence of operations such as outlining algorithm, filtering outer and small rings, and the flood fill algorithm, the segmented image is obtained. The explained process is presented in Figure 1.

Like the image shown in this figure, the nodules connected to the lung wall are probably not separated correctly. In order to consider those areas, instead of only considering the segmented area, a box containing this area with a margin of 10 pixels for the outer sides is considered as a mask. By applying this mask to the original image, the lung corpus is obtained. The generated corpora are used as the input to the model.

The architecture of the proposed lung nodule detection using CT image is diagrammed in Figure (2). Three parts can be seen in the proposed architecture; 1) convolutional feature extraction, 2) feature fusion, and 3) multi-task learning. In the test phase, at the end, non-maximum suppression is performed as a post-processing step.

The first part is convolutional feature extraction. It consists of nine convolutional layers and four max-pooling layers. In the next part, to capture nodules of multi-scales, the features extracted from three streams are combined after up-sampling. The obtained features are fed into a multi-task learning part. There are two branches in the training part: classification task and regression task.

The output of the classification task, Y , is a $h/4 \times w/4$ tensor, in which (h, w) is the dimension of the original image. Y can be obtained by down-sampling the segmentation between nodule and normal from the original image. A high score means that the pixel most likely belongs to the nodule category.

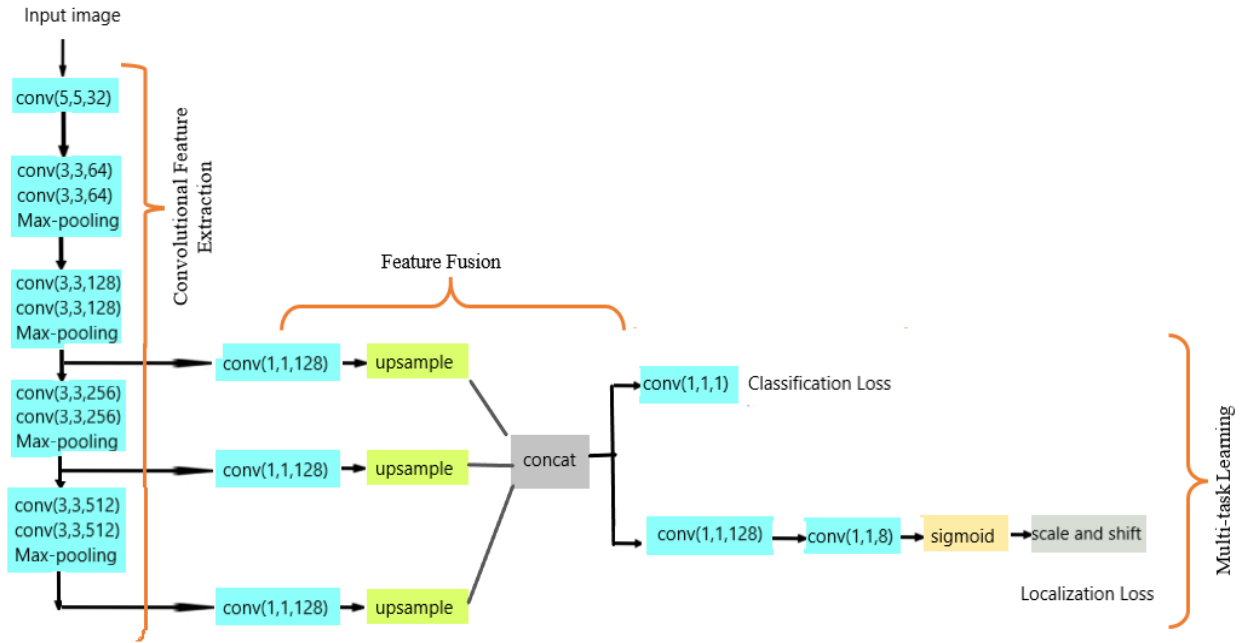


Figure 2. Structure of the proposed architecture for nodule detection.

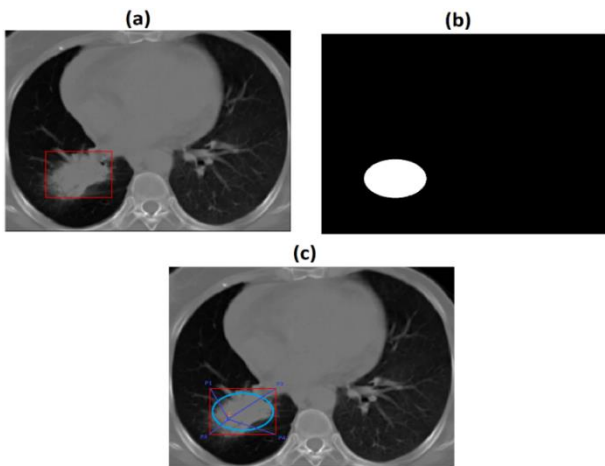


Figure 3. (a) A sample CT scan with the ground truth. (b) Ground truth for classification task. (c) Generating ground truth for regression task.

The output of the regression task, Z , is a $h/4 \times w/4 \times 8$ tensor. For each pixel that belongs to the nodule area, the distances of the corners of the quadrilateral boundary of the nodule to that point are determined.

By considering the offset values as Z , the coordinates of the i th corner of the bounding box in the input image for pixel $[x, y]$ belonging to the positive area in the downsampled image can be obtained as:

$$corner_i[4x, 4y] = [4x + Z(x, y, 2i - 1), 4y + Z(x, y, 2i)] \quad (1)$$

The loss function used for training includes two terms (i.e. classification ($Loss_{cls}$), and regression

loss ($Loss_{loc}$)) and can be represented as Equation (2):

$$Loss = Loss_{cls} + \lambda Loss_{loc} \quad (2)$$

Here, λ is the weighting factor that controls the balance between two losses. The ground truth for the classification task is generated by down-sampling the segmentation between nodule and non-nodule from the input image.

Instead of considering all pixels within a bounding box as a nodule, we only regard the pixels around the center of the box as positive labels. To do so, we consider an ellipse that is enclosed by the bounding box. The area inside an ellipse that is a downscale of the original ellipse by a parameter 0.9 is considered as the positive area. As an example, a lung CT image with one bounding box that marks a nodule is shown in Figure 3. The ground truth of the classification task is also presented in this figure.

By considering $y_i^* \in \{0,1\}$ as the ground truth for i th pixel of the input image and \hat{y}_i as the predicted value, the classification loss can be obtained as:

$$Loss_{cls} = \frac{-1}{output_size} \sum_i y_i \log \hat{y}_i + (1 - y_i) \log(1 - \hat{y}_i) \quad (3)$$

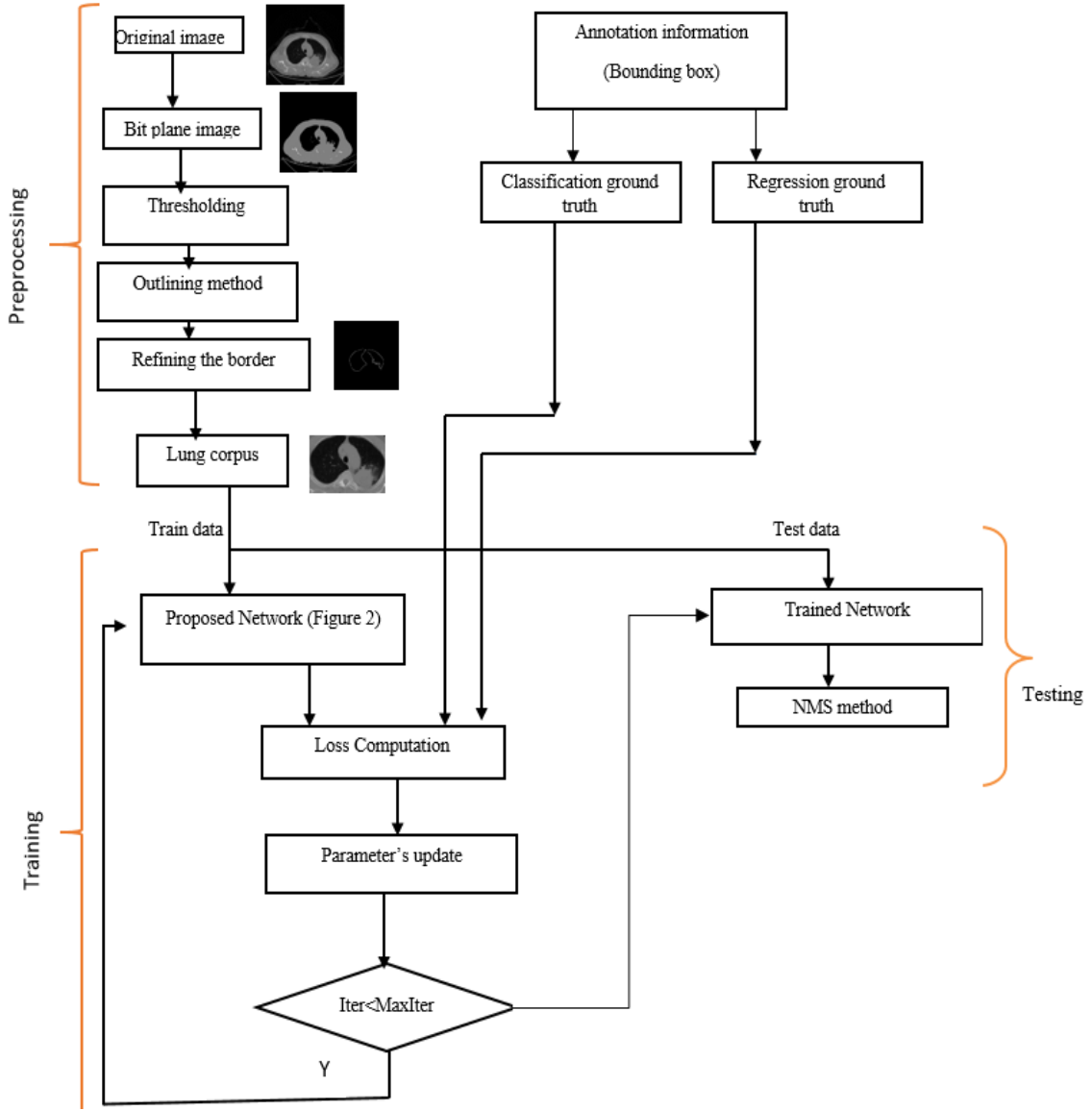


Figure 4. Block diagram of proposed framework

The ground truth of the regression task can vary over a wide range, so for a fast convergence, the scale and shift operation is used. The ground truth of the regression task is obtained as follows.

According to Figure 3.c, suppose that $P_1 = [P_{1,x}, P_{1,y}]$, $P_2 = [P_{2,x}, P_{2,y}]$, $P_3 = [P_{3,x}, P_{3,y}]$, $P_4 = [P_{4,x}, P_{4,y}]$ are the four coordinates of the quadrilateral containing the tumor in the original image. Consider pixel C with coordinate $[C_x, C_y]$, which belongs to the positive area. The following equation is used to generate the ground truth.

$$Z[C_x, C_y, 2i - 1 : 2i] = \left[\frac{P_{i,x} - C_x}{w}, \frac{P_{i,y} - C_y}{h} \right], \quad i = 1, 2, 3, 4 \quad (4)$$

As mentioned earlier, the output of the regression task is a tensor with shape $h/4 \times w/4 \times 8$. By considering P'_i as the i th

corner of the bounding box in the down-sampled image and $P_i = 4P'_i$, the ground truth for the down-sampled image can be obtained.

On the other hand, scale and shift operation can be used as follows in order to make the final output to be in the range of $(-1, 1)$:

$$\hat{Z} = 2Z' - 1 \quad (5)$$

in which, Z' is the output of the last layer after passing a sigmoid activation function.

By considering \hat{Z} and Z as the network's output and the ground truth, respectively, the regression loss can be formulated as:

$$Loss_{loc} = \sum_{i=1}^8 \sum_{p \in \text{positive_area}} \exp(|Z_p[i] - \hat{Z}_p[i]|) \quad (6)$$

According to the proposed architecture, for each point in the output map a scored bounding quadrilateral is obtained. The high-scored points are preserved for classification and bounding quadrilateral estimation. However, at some positions, there are still several overlapped quadrilaterals. In order to filter out the best bounding boxes, the non-maximum suppression method (NMS) can be used. The intersection over the union (IoU) metric can be used as an appropriate selecting measure. IoU is usually used to quantify the percent overlap between two bounding boxes. It can be represented as:

$$IoU(B_1, B_2) = \frac{\text{intersection-size}(B_1, B_2)}{\text{union-size}(B_1, B_2)} \quad (7)$$

In the NMS method, first of all, a list of quadrilaterals with scores higher than a confidence score is created. In each iteration, a box with the highest score is removed from the list and is added to the desired filtered output. Then the boxes with a high IoU with the removed box are also removed from the list. This process is repeated until the list is empty.

Since for each image belonging to the database used only one bounding box is specified, it seems that there is no need to use the NMS method. However, here, in order to calculate FP for a better evaluation, the NMS method is applied on the quadrilateral with a score higher than a confidence score. The block diagram is shown in Figure 4 shows an overview of the proposed framework.

3. Experimental Results

Here, in order to evaluate the proposed nodule detection method, the Lung-PET-CT-DX dataset is used [34]. This dataset contains 512×512 CT Dicom images of Lung cancer, subject with the XML annotation files for each CT image. The nodule's location is indicated with a bounding box. The annotation of each tumor is performed by five thoracic radiologists with expertise in lung cancer. Some examples of lung CT scans with their bounding boxes that mark the nodules are presented in Figure 5. Here, the images of 235 patients are used to evaluate the proposed method. 1480 images belonging to 19 patients are considered as the test set and 11504 scans belonging to 216 patients are considered as a train set.

As mentioned, for each image, only one bounding box is specified as the nodule location. Here, the proposed method is evaluated from two

aspects. In both aspects, a detected bounding box is considered a true positive (TP) if its IoU with the ground-truth is greater than a threshold and its confidence score is greater than a threshold. Violation of either of these two conditions makes a false positive (FP). A detected bounding box whose confidence score is lower than a threshold while it is supposed to detect a ground truth is considered as a false negative (FN). A detected bounding box whose confidence score is lower than a threshold while it is not supposed to detect a ground truth counts as a true negative (TN). TN is usually not considered in the evaluation for object detection applications. The two aspects are as follows:

- Aspect 1: All the obtained quadrilaterals after applying the NMS method are treated as a nodule. It is clear that the number of FNs is decreased while the number of FPs is increased.
- Aspect 2: Only a quadrilateral with the highest score is considered as a nodule. Here, the number of FNs is increased while the number of FPs is decreased. It has to be noted that rejecting true positives can be fatal.

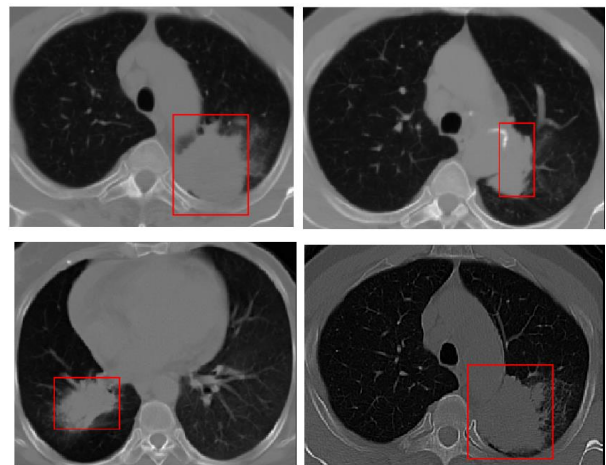


Figure 5. A few examples of lung CT scans along with ground truth.

Figure 6 shows examples of the output of the proposed method. In this figure, some CT scans in which more than a single nodule is detected are presented. Here, the bounding boxes that contain correctly the recognized nodules are marked in purple.

For a better evaluation, recall and precision are used. These metrics can be obtained as Equations (8) and (9) [35].

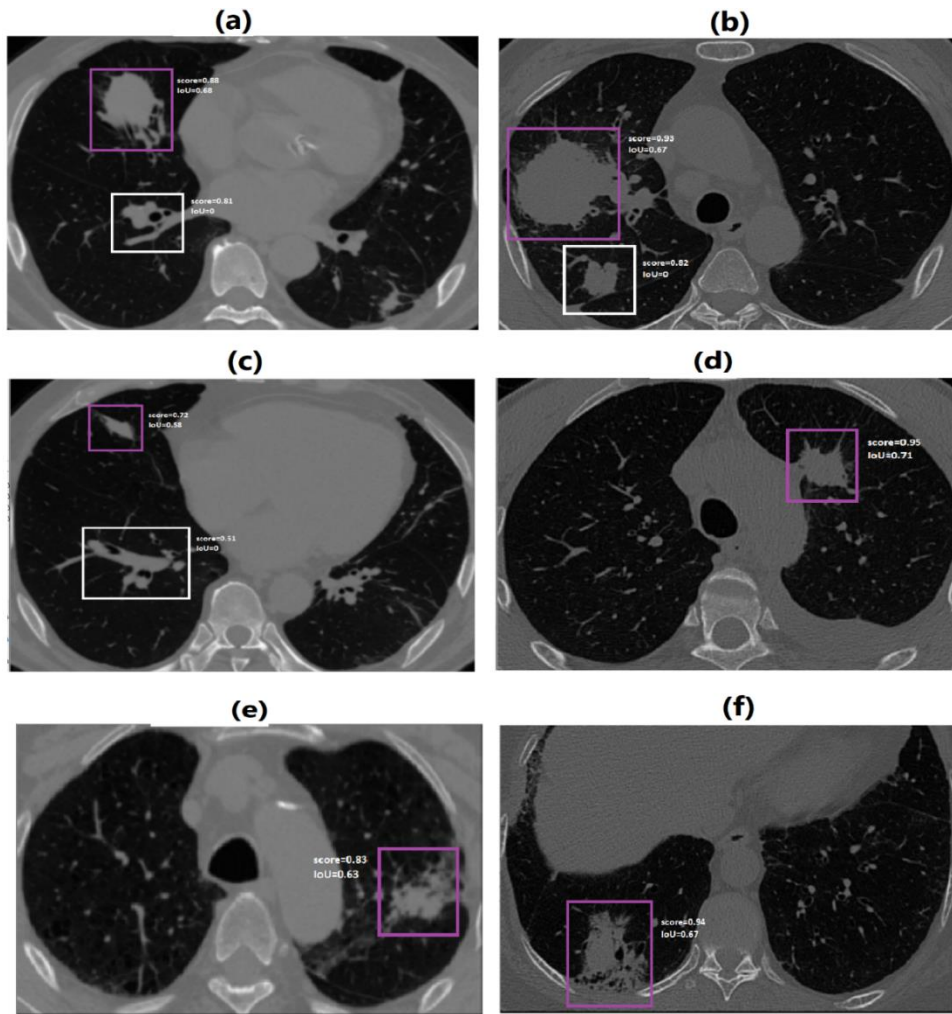


Figure 6. Detection results randomly chosen from test set. Correct predictions and FPs are marked with purple and white solid boxes, respectively. Numbers beside predictions are confidence scores and IoU with ground-truth.

$$\text{Precision} = \frac{TP}{TP + FP} \quad (8)$$

$$\text{Recall} = \frac{TP}{TP + FN} \quad (9)$$

The results of considering each strategy are described in Table 1.

It seems that the second aspect performs statistically better than the first aspect but for practical approaches, the first aspect is better than the second one because FN can have bad consequences for the patients. Moreover, a comparison between the proposed method and the YOLOv2-based nodule detection method is presented in Table 1.

Table 1. Evaluation of nodule detection.

| | | TP | FP | FN | Precision % | Recall % |
|------|---------|------|-----|-----|-------------|----------|
| P.M | Aspect1 | 1297 | 319 | 183 | 80.25 | 87.63 |
| | Aspect2 | 1201 | 226 | 279 | 84.16 | 81.15 |
| YOLO | Aspect1 | 1191 | 325 | 289 | 78.56 | 80.47 |
| V2 | Aspect2 | 1120 | 261 | 360 | 81.1 | 75.68 |

It can be observed that the proposed method outperforms this method.

4. Conclusion

In this paper, a deep-learning-based framework for nodule detection on lung CT scans was proposed. First, the background and some irrelevant parts of images were removed using a bit-plane-based segmentation algorithm. Then the obtained corpora were fed into a CNN-based model. The output of the model has two branches: classification and regression tasks. The regression task was performed using a direct approach. The NMS algorithm was used as a post-processing step in order to filter out the best bounding boxes. For evaluation, the Lung-Pet-CT-DX database was utilized. According to the searches in recent studies, this is apparently the first time this data has been used in learning-based nodule detection. Moreover, the performance of the proposed method was compared with the YOLOv2 method. By considering the bounding

boxes with the highest score as nodules, out of 1480 nodules, 1201 nodules were recognized correctly.

References

- [1] D. Arenberg, "Update on screening for lung cancer", *Transl. Lung Cancer Res.*, vol. 8, pp. 77-87, 2019.
- [2] W. J. Choi and T. S. Choi, "Automated pulmonary nodule detection based on three-dimensional shape-based feature descriptor". *Comput. Methods Programs Biomed.*, vol.113, pp. 37-54, 2014.
- [3] A. O. F. de Carvalho, W. B. de Sampaio, A. C. Silva, A. C. de Paiva, R. A. Nunes, and M. Gattass, "Automatic detection of solitary lung nodules using quality threshold clustering, genetic algorithm and diversity index". *Artif. Intell. Med.*, vol. 60, pp. 165-177, 2014.
- [4] T. Adams, J. Drpinghaus, M. Jacobs, and V. Steinhage, "Automated lung tumor detection and diagnosis in CT scans using texture feature analysis and SVM". *Communication Papers of the Federated Conference on Computer Science and Information Systems*, pp. 13–20, 2018.
- [5] O. Zinoveva, D. Zinovev, S. A. Siena, D. S. Raicu, J. Furst, and S. G. Armato, "A texture-based probabilistic approach for lung nodule segmentation". *In International Conference Image Analysis and Recognition*, pp. 21-30. Springer, Berlin, Heidelberg, June 2011.
- [6] A.C. Jirapatnakul, S. V. Fotin, A. P. Reeves, A.M. Biancardi, D. F. Yankelevitz, and C. I. Henschke, C. I." Automated nodule location and size estimation using a multi-scale Laplacian of Gaussian filtering approach." *Annual International Conference of the IEEE Engineering in Medicine and Biology Society*, pp. 1028-1031, IEEE, 2009.
- [7] Y. Tao, L. Lu, M. Dewan, A. Y. Chen, J. Corso, J. Xuan, and A. Krishnan, "Multi-level ground glass nodule detection and segmentation in CT lung images". *International Conference on Medical Image Computing and Computer-assisted Intervention*, pp. 715-723, Springer, Berlin, Heidelberg, September 2009.
- [8] K. Murphy, B. van Ginneken, A. M. Schilham, B. J. De Hoop, H. A. Gietema, and M. Prokop, "A large-scale evaluation of automatic pulmonary nodule detection in chest CT using local image features and k-nearest-neighbor classification". *Med. Image Anal.*, vol. 13, pp. 757-770, 2009.
- [9] J. K. Liu, H. Y. Jiang, M. D. Gao, C. G. He, C. G., Y. Wang, P. Wang, and H. Ma, "An assisted diagnosis system for detection of early pulmonary nodule in computed tomography images". *J. Med. Syst.*, vol. 41, pp. 1-9, 2017.
- [10] W. Huang, Y. Xue, and Y. Wu, "A CAD system for pulmonary nodule prediction based on deep three-dimensional convolutional neural networks and ensemble learning". *Plos one*, vol. 14, 2019.
- [11] w. Li, P. Cao, D. Zhao, and J. Wang, "Pulmonary nodule classification with deep convolutional neural networks on computed tomography images". *Comput. Math. Methods Med.*, vol. 2016, 2016.
- [12] A. Ray, "Lung Tumor Segmentation via Fully Convolutional Neural Networks", 2016.
- [13] H. Cao, H. Liu, H., E. Song, G. Ma, X. Xu, R. Jin, and C. C. Hung, "A two-stage convolutional neural networks for lung nodule detection". *IEEE J. Biomed. Health Inform.* vol. 24, pp. 2006-2015, 2020.
- [14] R. Girshick, J. Donahue, T. Darrell, and J. Malik, "Region-based convolutional networks for accurate object detection and segmentation". *IEEE Trans. Pattern Anal. Mach. Intell.*, vol. 38, pp. 142-158, 2015.
- [15] R. Girshick, "Fast r-cnn". *In Proceedings of the IEEE international conference on computer vision*, pp. 1440-1448, 2015.
- [16] S. Ren, K. He, R. Girshick, and J. Sun, "Faster r-cnn: Towards real-time object detection with region proposal networks". *Adv. Neural Inf. Process. Syst.*, 28, pp. 91-99, 2015.
- [17] K. He, G. Gkioxari, P. Dollr, and R. Girshick, "Mask r-cnn". *In Proceedings of the IEEE international conference on computer vision*, pp. 2961-2969, 2017.
- [18] S. Kido, Y. Hirano, and N. Hashimoto, "Detection and classification of lung abnormalities by use of convolutional neural network (CNN) and regions with CNN features (R-CNN)". *In 2018 International workshop on advanced image technology (IWAIT)*, pp. 1-4, IEEE, January 2018.
- [19] J. Ding, A. Li, Z. Hu, and L. Wang, "Accurate pulmonary nodule detection in computed tomography images using deep convolutional neural networks". *In International Conference on Medical Image Computing and Computer-assisted Intervention*, pp. 559-567, Springer, Cham, September 2017.
- [20] W. Zhu, C. Liu, W. Fan, and X. Xie, "Deeplung: Deep 3d dual-path nets for automated pulmonary nodule detection and classification". *In 2018 IEEE Winter Conference on Applications of Computer Vision (WACV)*, pp. 673-681, IEEE, March 2018.
- [21] Z. Xie, "3D region proposal u-net with dense and residual learning for lung nodule detection". *LUNA16*, 2017.
- [22] Y. Su, D. Li, and X. Chen, "Lung nodule detection based on faster R-CNN framework", *Comput. Methods Programs Biomed.*, vol. 200, 2021.
- [23] H. Xie, D. Yang, N. Sun, Z. Chen, and Y. Zhang, "Automated pulmonary nodule detection in CT images

using deep convolutional neural networks”. *Pattern Recognit.*, vol. 85, pp. 109-119, 2019.

[24] E. R. Capia, A. M. Sousa, and A. X. Falco, “Improving lung nodule detection with learnable non-maximum suppression”, *In 2020 IEEE 17th International Symposium on Biomedical Imaging (ISBI)*, pp. 1861-1865, IEEE, 2020.

[25] H. Tang, D. R. Kim, and X. Xie, “Automated pulmonary nodule detection using 3D deep convolutional neural networks”, *In 2018 IEEE 15th International Symposium on Biomedical Imaging (ISBI 2018)*, pp. 523-526, IEEE, April 2018.

[26] L. Cai, T. Long, Y. Dai, and Y. Huang, “Mask R-CNN-based detection and segmentation for pulmonary nodule 3D visualization diagnosis”. *IEEE Access*, vol. 8, pp. 44400-44409, 2020.

[27] M. Liu, J. Dong, X. Dong, H. Yu, and L. Qi, “Segmentation of lung nodule in CT images based on mask R-CNN”, *In 2018 9th International Conference on Awareness Science and Technology (iCAST)*, pp. 1-6, IEEE, September 2018.

[28] W. Fan, H. Jiang, L. Ma, J. Gao, and H. Yang, “A modified faster R-CNN method to improve the performance of the pulmonary nodule detection”. *In 10th International Conference on Digital Image Processing (ICDIP 2018)* (Vol. 10806, p. 108065A). International Society for Optics and Photonics, August 2018.

[29] N. Guo, and Z. Bai, “Multi-scale Pulmonary Nodule Detection by Fusion of Cascade R-CNN and FPN”. *In 2021 International Conference on Computer Communication and Artificial Intelligence (CCAI)*, pp. 15-19, IEEE, May 2021.

[30] J. George, S. Skaria, and V. Varun, “Using YOLO-based deep learning network for real-time detection and localization of lung nodules from low dose CT scans”. *In Medical Imaging 2018: Computer-Aided Diagnosis International Society for Optics and Photonics*, p. 105751, February 2018.

[31] L. Xinzheng, J. Wei, L. Gang, and Y. Caoqian, “YOLO V2 Network with Asymmetric Convolution Kernel for Lung Nodule Detection of CT Image”. *Chinese Journal of Biomedical Engineering*, 2019.

[32] L. Haibo, T. Shanli, S. Shuang, and L. Haoran, “An improved yolov3 algorithm for pulmonary nodule detection”. *In 2021 IEEE 4th Advanced Information Management, Communicates, Electronic and Automation Control Conference (IMCEC)*, Vol. 4, pp. 1068-1072, IEEE, June 2021.

[33] W. He, X. Y. Zhang, F. Yin, and C. L. Liu, “Multi-oriented and multi-lingual scene text detection with direct regression”, *IEEE Trans. Image Process.*, vol. 27, pp. 5406-5419, 2018.

[34] A Large-Scale CT and PET/CT Dataset for Lung Cancer Diagnosis (Lung-PET-CT-Dx) The Cancer Imaging Archive (TCIA) Public Access, Cancer Imaging Archive Wiki.

[35] J. Barazande, and N. Farzaneh, “WSAMLP: Water Strider Algorithm and Artificial Neural Network-based Activity Detection Method in Smart Homes”. *Journal of AI and Data Mining*, 2021.

تشخیص خودکار ندول‌های ریه در اسکن توموگرافی کامپیوتری با روش رگرسیون مستقیم عمیق

خدیجه آقاجانی*

دانشکده مهندسی کامپیوتر، دانشگاه مازندران، بابلسر، ایران

ارسال ۲۰۲۱/۱۲/۰۲؛ بازنگری ۲۰۲۱/۱۲/۲۶؛ پذیرش ۲۰۲۲/۰۲/۰۵

چکیده:

رویکردهای مبتنی بر یادگیری عمیق به طور گسترده در تشخیص ندول‌های ریوی با استفاده از اسکن‌های توموگرافی کامپیوتری مورد استفاده قرار می‌گیرند. در این کار، یک چارچوب خودکار انتها به انتها با یک شبکه کانولوشن (Conv-net) برای تشخیص ندول‌های ریه از تصاویر CT پیشنهاد شده‌است. در اینجا رگرسیون مرزی با روش رگرسیون مستقیم انجام شده است که در آن افست از یک نقطه معین پیش‌بینی می‌شود. چارچوب پیشنهادی دو خروجی دارد. یک طبقه بندی پیکسلی جهت تشخیص ندول و یا نرمال بودن هر نقطه و یک رگرسیون مستقیم که به منظور تعیین مختصات چهار ضلعی دور ندول استفاده می‌شود. تابع هزینه شامل دو عبارت است. یکی برای طبقه بندی و دیگری برای رگرسیون. عملکرد روش پیشنهادی با YOLOv2 مقایسه شده است. ارزیابی با استفاده از مجموعه داده Lung-Pet-CT-DX انجام می‌شود. نتایج تجربی نشان می‌دهد که چارچوب پیشنهادی بهتر از روش YOLOv2 عمل می‌کند. نتایج به دست آمده نشان می‌دهد که چارچوب پیشنهادی دارای دقت بالایی در مکان‌یابی ندول و تخمین مرز است.

کلمات کلیدی: تشخیص ندول ریه، رگرسیون مستقیم، یادگیری عمیق.